Int. J. Electrochem. Sci., 16 **(2021)** 151024, doi: 10.20964/2021.01.48

International Journal of
ELECTROCHEMICAL
SCIENCE
www.electrochemsci.org

State of Charge and Lithium Manganate Batteries Internal Resistance Estimation at Low Charge/discharge rates

Xiongping Lin[1,2], *Jieqing Zheng*[1,*], *Zheng Zou*[1,*], *Feng Lin*[1], *Dingrong Deng*[1], *Chunyan Cao*[1], *Xin Wen*[1], *Linhua Que*[1] *and Juqiong Yang*[1]

[1] Cleaning Combustion and Energy Utilization Research Center of Fujian Province (Jimei University), Xiamen 361021, PR China
[2] Chengyi College, Jimei University, Xiamen 361021, PR China
[*]E-mail: zhjieqing@126.com, xxzz6670@jmu.edu.cn

Received: 10 September 2020 / *Accepted:* 7 November 2020 / *Published:* 30 November 2020

Several parameters relating to electric vehicles vary with the state of charge (SOC). In currently commonly used equivalent circuit models, changes of the Ohmic resistance (R_0) and polarization resistance (R_p) during charge and discharge are ignored. Therefore, the models only present high accuracy on specific conditions, which cannot replicate the dynamic characteristics of lithium ion batteries. Parameter identification was performed on open circuit voltage (OCV) and direct-current internal resistance by employing the hybrid pulse power characterization (HPPC) method to improve calculation accuracy. The test result shows that the Ohmic resistance and the total internal resistance are influenced by the rate and the OCV and polarization resistance are significantly affected by the SOC; at different SOCs, the larger the charge and discharge rates are, the larger the polarization resistance of a battery (correspondingly, the greater the change to the curve) and the lower the Ohmic resistance and the total internal resistance of the battery (the less significant the change to their curves).

Keywords: Ohmic resistance, polarization resistance, hybrid pulse power characteristics.

1. INTRODUCTION

Electric vehicles, effectively replacing traditional fossil fuels, are being developed worldwide. The real-time and accurate monitoring of the state of charge (SOC) is indispensable for exploring the power system performances and guaranteeing the operational reliability of electric vehicles; however, electric vehicles run in a complex and varying operating environment and their various parameters change with the SOC [1,2]. This causes the battery performance to show a strongly non-linear dynamic relationship, making calculation of the SOC difficult. As one of important performance parameters of a battery, the internal resistance of batteries includes polarization resistance (R_p) and Ohmic resistance

(R_0) [3, 4]. In the commonly used equivalent circuit model, changes of the Ohmic resistance and polarization resistance during the charge and discharge are ignored. Therefore, the model only delivers high accuracy under specific conditions, and fails to replicate the dynamic characteristics of lithium (Li) ion batteries [5].

The internal resistance of a battery is an important parameter for judging the aging condition thereof. The Ohmic resistance consists of contact resistances of various parts such as electrode, electrolyte, separator, and current collector, which is influenced by many factors, *e.g.* ambient temperature, electrolyte concentration and the structure of active substances. The internal reaction is generally non-linear [6, 7]. Polarization resistance refers to the impedance caused by the electric potential in positive and negative electrodes deviating from thermodynamic equilibrium to the passage of Li ions, and it fluctuates under the effects of the SOC and charging and discharging powers [8]. After a long-term charge and discharge, the positive and negative poles of a battery are corroded, influencing the concentration and viscosity of the electrolytes. In addition, the reduction of the active substances in the battery impairs Li ion and electron conduction, which leads to the decrease of the electrochemical reaction rate, aging of the battery and increase of its internal resistance. Moreover, the internal resistance of a battery will also vary due to a series of factors including adverse ambient operating temperature, over-charge and over-discharge, and high-current charge and discharge [9-11]. Liu *et al.* [12] found that the internal resistance increases with decreasing temperature by exploring the change in the internal resistance of $LiCoO_2$ ion batteries. Song *et al.* [13] showed that the internal resistance of Li ion batteries is affected by temperature and a thermal runaway accident will be induced at high temperature.

Accurately measuring the SOC can prevent a battery from being damaged due to over-charge and over-discharge; strengthen the management on its safety performance; prolong the service life of the battery; exploit the full potential of the battery, and avoid delivery of an insufficient electromotive force [14]. The main methods for calculating the SOC of a battery involve the discharge test, ampere-hour integration, and open circuit voltage (OCV) methods. In terms of the discharge test method, the SOC is described based on time and current when reaching the cut-off voltage through constant-current discharge. The method requires a long waiting time. The Ampere-hour integration method sets onerous requirements on the measurement accuracy of the current and the initial SOC. The OCV requires a certain functional relationship between the OCV and SOC, showing favorable estimation effect [15, 16].

The commonly used methods for testing the internal resistance involve the OCV, volt-ampere (V-A) characteristic curve, density and hybrid pulse power characterization (HPPC) methods. Compared to the other methods, the HPPC method can more accurately attain the direct-current internal resistance under the SOC through simple operation [17]. The parameters (*i.e.* U_{ocv}, R_0, and R_p) were identified by using the data obtained through HPPC test according to *Freedom CAR Battery Test Manual for Power-assisted Hybrid Electric Vehicles* [18, 19]. Furthermore, the relationships between the OCV and internal resistance with the SOC at different rates (0.1 C, 0.2 C, and 0.3 C) at constant-current charge and discharge modes were analyzed to obtain the relationships of the rate and SOC with the internal resistance. A low rate is used in the study. During charge and discharge cycling at a high rate, the internal temperature of batteries is high; the Li ion activity in the batteries rises and their diffusion rate increases, thus showing low Ohmic resistance.

2. BATTERY PERFORMANCE TEST

2.1 Test objects and equipment

The test was conducted by taking a CT-4008-5V20A-A high-accuracy test system for battery performance as the test platform and 106580 Lithium Manganate (LMO) batteries (produced by Shenzhen Kinne Power Company, with the rated voltage of 3.7 V and rated capacity of 4 Ah) with Al-plastic filmed case (soft packaging) as the research objects. Moreover, liquid electrolytes were used in the batteries, whose positive and negative electrodes separately were LMO and graphite. To prevent the test object from entering a protected mode during the charge and discharge cycle, the protection board was subjected to short-circuit processing before the test.

2.2 HPPC test of batteries

According to *Freedom CAR Battery Test Manual for Power-assist Hybrid Electric Vehicles* [18], the battery tests of electric vehicles were divided into performance test, life test and reference performance test, in which the HPPC test belongs to performance test. The HPPC method involves discharge for 10 s, shelving for 40 s, and feedback for 10 s. The HPPC method, despite its accuracy, suffers from error caused by the SOC during test response. Based on the HPPC method proposed in the manual, an applicable test method was proposed according to the equipment characteristics and the performance of the LMO batteries with 4 Ah.

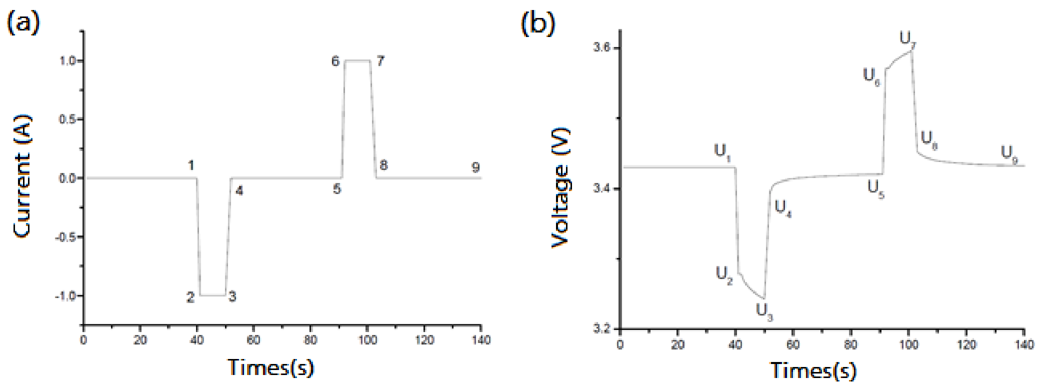

Figure 1. Testing principle underlying the HPPC method; discharging current as negative and charging current as positive; (a) current-time curve; (b) voltage-time curve.

At first, the batteries were shelved for 40 s before the HPPC test. The discharge pulse current was applied on the shelved batteries for 10 s and then the battery voltage decreased from U_1 to U_2. The voltage jump process was induced by the Ohmic resistance in the batteries. During discharge for 10 s, the voltage decreased slowly from U_2 to U_3, which was mainly caused by the polarization resistance. At the moment of ending the 10-s discharge, the voltage jumped from U_3 to U_4, which was also attributed to the Ohmic resistance; it was necessary to shelve the batteries for 40 s after the discharge, the voltage slowly increased from U_4 to U_5 during shelving, which was triggered by the polarization resistance; finally, the voltage stabilized at U_5. During a 10-s charge period, the voltage jump was similar. The OCV and internal resistance can be calculated by recording the voltages at various points in the curve in Fig. 1.

The OCV is calculated according the proposed method [20]. In the process of shelving the batteries for 40 s before and after the discharge process, the interior of the batteries was gradually rendered stable; the polarization effect was weakened and the polarization voltage was lowered; the voltage gradually stabilized. The currents were both zero at the end of shelving period at point 1 before, and at point 5 thereafter, the discharge and the internal polarization effect can be ignored. It can be stated that the polarization voltage is zero, thus, the mean voltages at points 1 and 5 are taken as the OCV. The internal resistance is calculated as follows:

Ohmic resistance during discharge	$R_{01} = (U_1 - U_2)/Ic$	(2-1)
	$R_{02} = (U_4 - U_3)/Ic$	(2-2)
	$R_0 = (R_{01} + R_{02})/2$	(2-3)
Polarization resistance during discharge	$Rp_1 = (U_2 - U_3)/Ic$	(2-4)
	$Rp_2 = (U_5 - U_4)/Ic$	(2-5)
	$Rp = (Rp_1 + Rp_2)/2$	(2-6)

where, Ic refers to the test current used in HPPC. According to low-current measurement in the test manual, 25% of the maximum allowable current during pulse discharge for 10 s stipulated by the manufacturer is selected as the test current during the HPPC test. The maximum current of the LMO batteries explored in the study during pulse discharge for 10 s stipulated by the manufacturer is 1 C (that is, 4 A), therefore, the pulse current is 1 A. The calculation of the Ohmic resistance and polarization resistance during charge is similar to that during discharge.

2.2 Test procedure

(1) At room temperature, the LMO batteries were first discharged to the lower limit of voltage, 3.0 V, at a constant current. In this case, the SOC was recorded as zero and then the batteries were shelved for 30 min;

(2) The batteries were charged for 30 min at a constant current (0.1 C, that is, 0.4 A) and the SOC rose to 0.05; afterwards, the batteries were shelved for 40 s and then discharged for 10 s at a constant current of 1 A; next, the batteries were charged for 10 s at a constant current of 1 A after being shelved for 40 s; subsequently, the batteries were shelved for 40 s again. In this way, a HPPC test was completed and the data were recorded every second;

(3) Two cycles were performed from Step (2) in each cycle. In this condition, the SOC increased to 0.1;

(4) While keeping other parameters unchanged, the charging time of 30 min in Step (2) was changed to 60 min. After performing eight cycles, the SOCs separately increased to 0.2, 0.3, 0.4, 0.5, 0.6, 0.7, 0.8, and 0.9.

(5) Through repeated operation according to the setting in Step (2), the SOC increased to 0.95.

(6) The batteries were charged for 30 min at a constant current (0.1 C) and therefore the SOC increased to 1.0.

(7) After completing the charge test, the batteries were shelved for 30 min and then also discharged at a constant current (0.1 C). According to Steps (2) to (6), the SOCs were separately adjusted to 0.95, 0.9, 0.8, 0.7, 0.6, 0.5, 0.4, 0.3, 0.2, 0.1, and 0.05 by setting corresponding time;

(8) The batteries were shelved for 30 min. At room temperature, the charge and discharge rates of the batteries were adjusted to 0.2 C and 0.3 C. Subsequently, the voltage changes at 0.2 C and 0.3 C were found by repeating Steps (2) to (7) and then the changes of the OCV and internal resistance during the charge and discharge can be attained through data processing.

3. RESULTS AND DISCUSSION

During the test, the current-time curve shapes during HPPC test under 0.1 C, 0.2 C, and 0.3 C are same as the voltage-time curve shapes. By taking the condition under 0.3 C as an example, the HPPC test is performed on the current and voltage at the SOC interval of 0.05 or 0.1 during charge and discharge. During the test, the charge and discharge capacities are both at about 0.2 Ah or 0.4 Ah. Moreover, the results obtained through the HPPC test in the figure are enlarged. The changes of the charging and discharging voltages, current, and capacity with time are shown in Fig. 2.

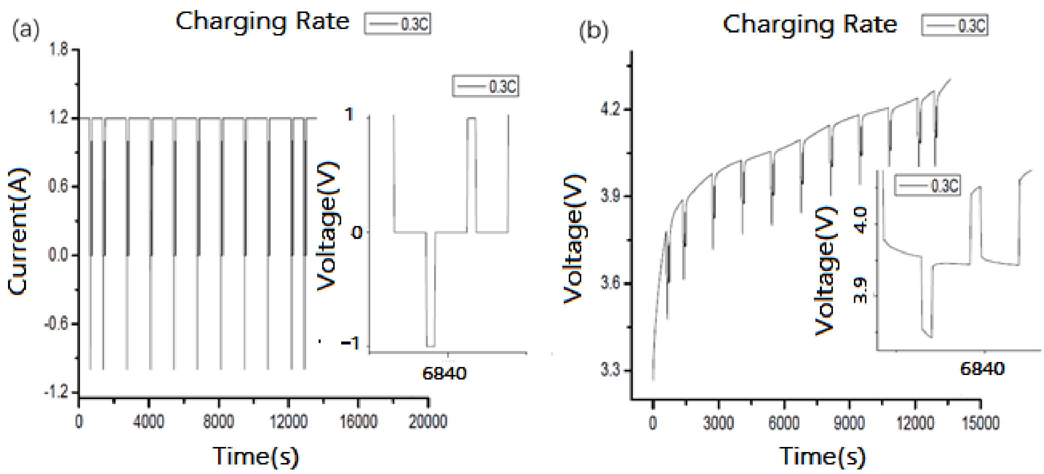

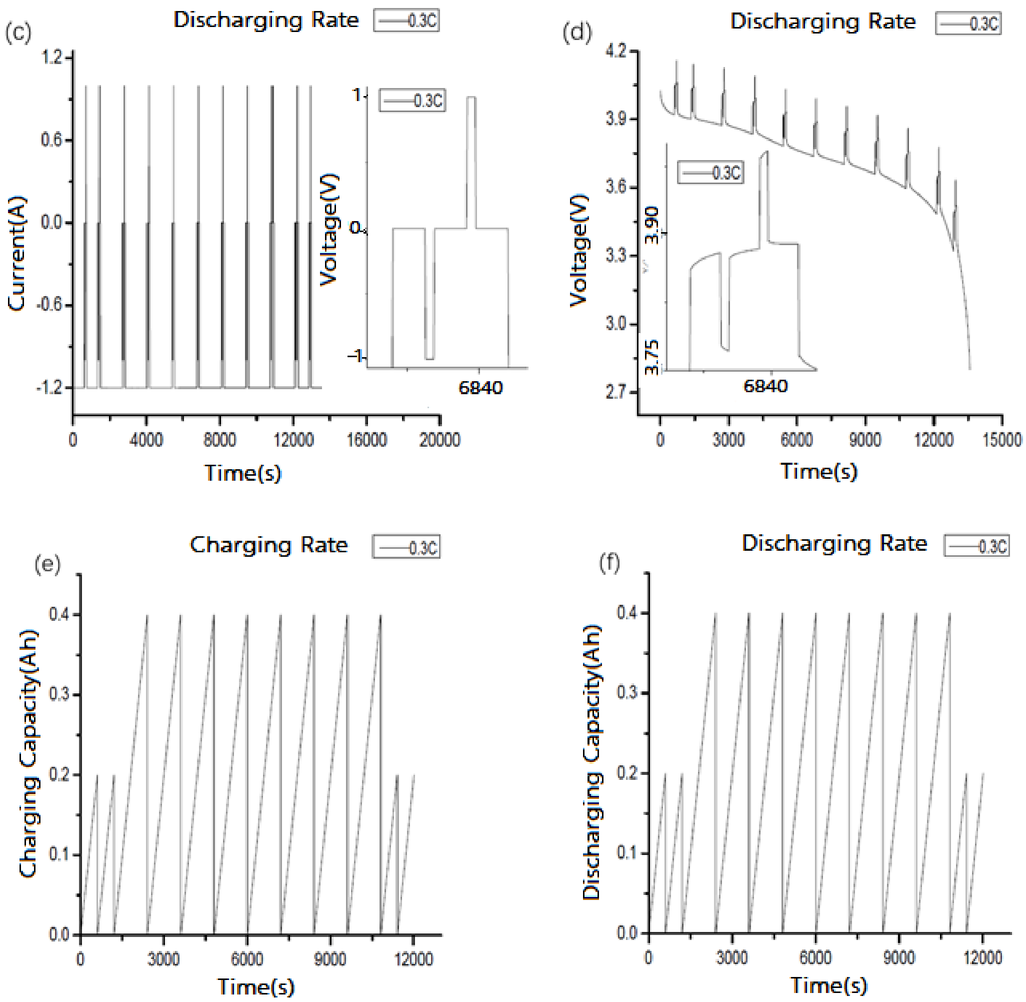

Figure 2. Charge and discharge tests through the HPPC method; (a) charging current; (b) charging voltage; (c) discharging current; (d) discharging voltage; (e) the change in charge capacity with time; (f) the change in discharge capacity with time.

3.1 Change in the OCV

When applying different rates during charge and discharge of a battery, the active substances in the battery are in different states and thereby react at different rates. As a result, the changes of the OCV and internal resistance vary. By processing the data obtained through testing at 0.1 C, 0.2 C, and 0.3 C, the changes in OCV, Ohmic resistance, polarization resistance, and total internal resistance with the SOC are acquired. The changes in OCV during charge and discharge with the SOC are shown in Fig. 3.

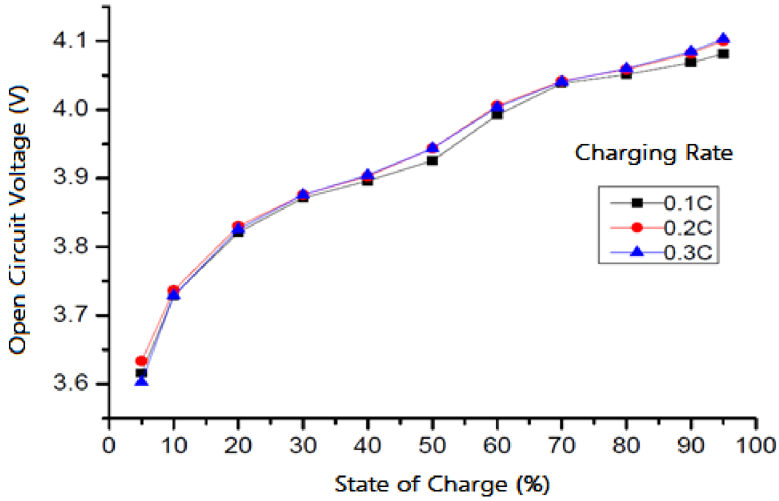

Figure 3. OCV-SOC curves during charging

Figure 3 shows that, as the charge continues, the OCV increases in a non-linear manner with increasing SOC (the change is staged). From 0.05 SOC to 0.3 SOC and 0.5 SOC to 0.6 SOC, the OCV increases rapidly. During the rapid growth of the OCV, there is also a significant difference at different rates and the difference of the OCV increases upon completion of charging.

The change of the OCV with the SOC during discharge is shown in Fig. 4.

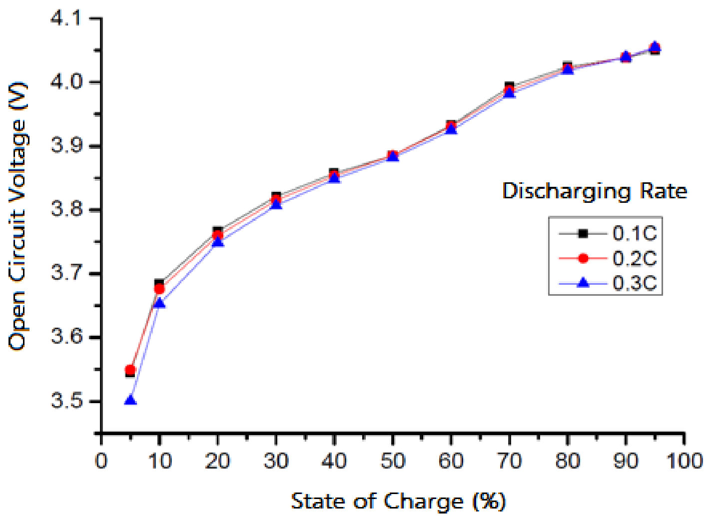

Figure 4. OCV-SOC curves during discharging

As shown in the figure, the larger the rate, the lower the OCV under the same SOC. In the initial discharge stage with 0.8 SOC to 0.95 SOC, the OCVs are similar at different rates. As the discharge continues, the OCV difference at different rates gradually increases; at the end of discharge stage with 0.05 SOC to 0.2 SOC, the OCV decreases rapidly. Generally, the OCV varies with the SOC and it is less significantly affected by the rate of charge.

The battery performances during charge and discharge differ slightly: a comparison of the OCV during charge and discharge at 0.3 C is shown in Fig. 5.

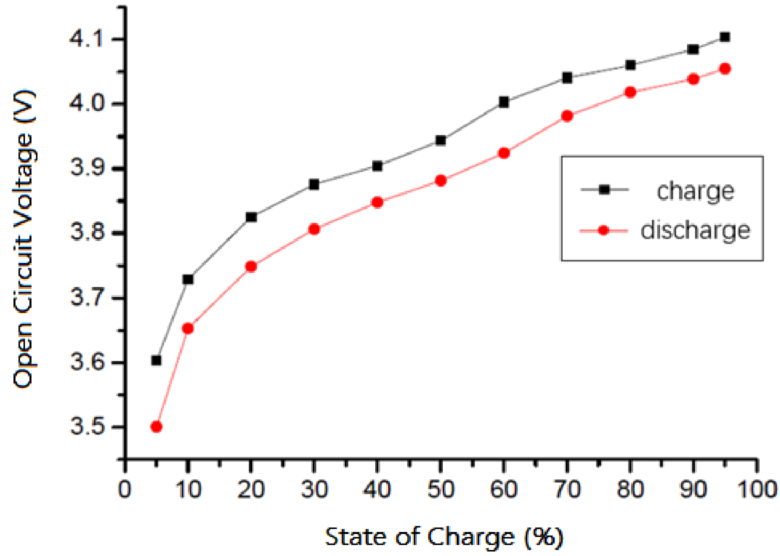

Figure 5. Relationship between OCV and SOC during charging and discharging at 0.3 C

As shown in the figure, the changes in OCV with the SOC are similar during charge and discharge. The difference only lies in that at the same SOC, the OCV during charging is always higher than that when discharging [21]. The difference of OCVs during the charge and discharge is attributed to the presence of the hysteresis effect [22]. The structures of the active substances in positive and negative electrodes during the charge and discharge present a certain difference, thus leading to different electromotive forces. Therefore, the OCVs are different during the charge and discharge at the same SOC. In addition, after the batteries are shelved, the working voltage when charging will decrease while that when discharging increases. Only when the batteries are shelved for sufficient time did the working voltage correspond to the OCV. Even if batteries are shelved for a long time before testing, the OCV when charging remains higher than that when discharging.

3.2 Changes in Ohmic resistance

There are different Ohmic resistances at different charge and discharge rates. The changes in Ohmic resistance during the charge and discharge phases are illustrated in Figs 6 and 7.

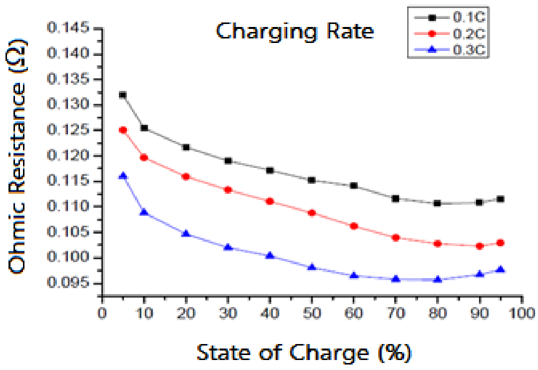

Figure 6. Ohmic resistance-SOC curves during charging

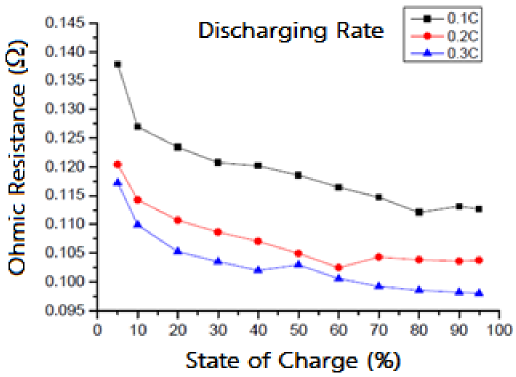

Figure 7. Ohmic resistance-SOC curves during discharging

When charging, the Ohmic resistance tends to decrease with increasing SOC. It is worth noting that the Ohmic resistance changes faster in the initial charging period and gradually rises in the final period.

At different charge rates, the Ohmic resistances differ significantly: at 0.1 C, 0.2 C, and 0.3 C, the ranges of the Ohmic resistance are 20.3, 22.8, and 20.5 mΩ, respectively. The possible reason is that during the high-rate charge, the formation rate of the solid electrolyte interphase (SEI) film is lower than its decomposition rate. Furthermore, the SEI film is decomposed and thinned, and reaches a new equilibrium in the batteries, thus having a low resistance [23].

The relationship between the Ohmic resistance and the SOC during the discharge is akin to that when charging. At the end of the discharge process, the Ohmic resistance is changed by more than that when charging at the same SOC.

3.3 Changes of polarization resistance

It can be seen from the test principle underlying the HPPC method in Fig. 1 that the discharging current is applied on the batteries and the terminal voltage slowly decreases from U_2 to U_3 section: in this stage, the RC parallel circuit shows the zero-state response. The charging current also influences the polarization resistance. The changes in polarization resistance with the SOC during charge and discharge at different rates are shown in Figs 8 and 9.

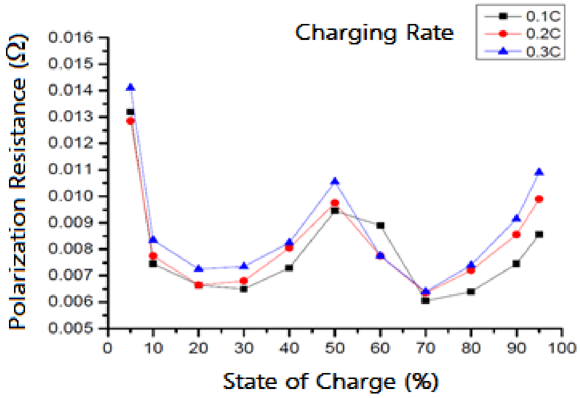

Figure 8. Polarization resistance-SOC curves during charging

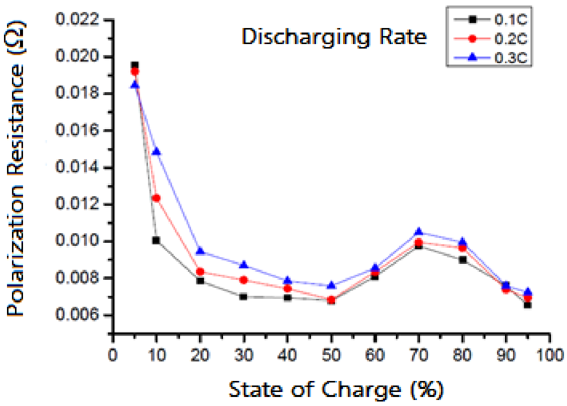

Figure 9. Polarization resistance-SOC curves during discharging

The SOC-polarization resistance curves when charging are ω-shaped: from SOC = 0.05 to 0.2, the polarization resistance decreases: the largest change occurs from 0.05 SOC to 0.1 SOC; from 0.2 SOC to 0.5 SOC, the polarization resistance gradually increases, while decreasing from 0.5 SOC to 0.7 SOC; the polarization resistance increases from 0.7 SOC to 0.95 SOC; the polarization resistances are large at the beginning (0.05 SOC), in the middle (0.5 SOC), and end (0.95 SOC) of the charging phase.

The polarization resistance varies with the SOC. Under the effect of different Li ion concentration differences around positive and negative electrodes, the polarization resistance is higher during high-rate charging; however, there is an insignificant difference in the polarization resistance at different rates [18].

In the initial discharge stage (0.7 SOC to 0.95 SOC), the polarization resistance increases while it decreases from 0.5 SOC to 0.7 SOC; it increases from 0.05 SOC to 0.5 SOC. The minimum and maximum polarization resistances separately occur at 0.95 SOC and 0.05 SOC, that is, the polarization resistance is minimized upon initial discharge. When reaching the end of the discharge phase, the polarization resistance reaches a maximum at 0.05 SOC. From 0.05 SOC to 0.3 SOC and 0.6 SOC to 0.9 SOC, the polarization resistance during discharge exceeds that during charging while the former is lower than the latter from 0.3 SOC to 0.6 SOC and 0.9 SOC to 0.95 SOC.

3.4 Changes in total internal resistance

The total internal resistance is equal to the sum of the polarization resistance and Ohmic resistance (Figs 10 and 11). It can be seen from the figures that the lower the rate of charge, the higher the total internal resistance and the less significant the reduction. throughout the charging stage, the change of the total internal resistance can be divided into four stages: the total internal resistance presents a large reduction from 0.05 SOC to 0.1 SOC; the change in total internal resistance decreases slightly, and at a decreasing rate, from 0.1 SOC to 0.5 SOC; the total internal resistance decreases significantly from 0.5 SOC to 0.7 SOC; from 0.7 SOC to 0.95 SOC, the total internal resistance starts to increase, and the larger the rate of change, the greater the amplitude. There are large resistances measured at 0.05 SOC, 0.5 SOC, and 0.95 SOC.

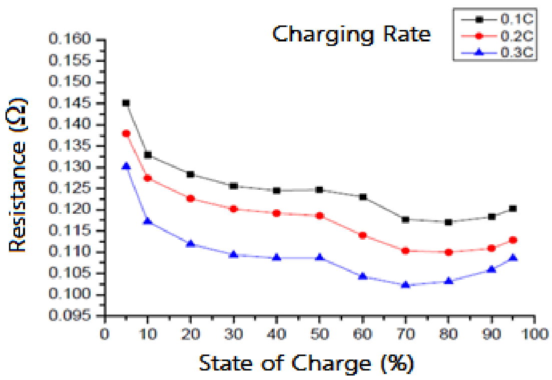

Figure 10. Total internal resistance-SOC curves during charging

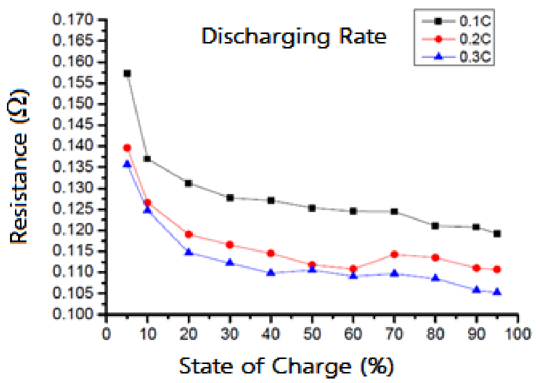

Figure 11. Total internal resistance-SOC curves during discharging

The change in total internal resistance with the SOC is similar to that in Ohmic resistance during discharge. The total internal resistance is affected by the charge and discharge rates: the faster the change, the lower the total internal resistance. Moreover, the total internal resistance decreases slightly with increasing SOC. At the same rate, the total internal resistance during discharge is always higher than that when charging, which is similar to the Ohmic resistance. The change of the polarization resistance is relatively complicated: under the synergistic effect of the Ohmic resistance and the internal resistance, the polarization resistance is most significantly changed between 0.05 SOC and 0.2 SOC.

4. CONCLUSION

At different rates, the changes in Ohmic resistance approach those of the total internal resistance during charging and discharging. The changes of the polarization resistance during charging and discharging differ greatly: the polarization resistances when charging and discharging are both large at the beginning and end of the charge and discharge cycle. The polarization resistances are the largest separately at 0.5 SOC and 0.7 SOC in the middle of the charge and discharge cycle. The larger the charge and discharge rates, the lower the Ohmic resistance and the total internal resistance; however, the larger the polarization resistances are during charging and discharging. The OCV and polarization resistances during the charge and discharge phases are unaffected while the Ohmic resistance and total internal resistance exhibit rate-dependence. Under different SOCs, the OCV, polarization resistance, Ohmic resistance, and total internal resistance during the charge and discharge cycle change to a significant extent, thus, it is thought that the main factors influencing the Ohmic resistance and the total internal resistance include the rate and SOC while those influencing the OCV and polarization resistance involve the SOC. Low rates (such as 0.1 C, 0.2 C, and 0.3 C) are used in the present study. When performing the charge and discharge by using a large rate, the internal temperature of the batteries is high; under such conditions, the Li ion activity in batteries rises and thus the rate of diffusion of ions increases, leading to a low resistance. The Ohmic resistance is therefore low at a high rate of charge.

ACKNOWLEDGEMENTS
Authors gratefully acknowledge financial support from the National Natural Science Foundation, Fujian Science and Technology Committee and Education Committee of China (project No.22005118, No. JK2016023 and No. JAS180220).

References

1. L.Y. Niu, P.R. Zhang and X.F. Wang, *J. Clean. Prod.,* 199(2018)1043.
2. R.F. Zhang, B.Z. Xia, B.H. Li, L.B. Cao, Y.Z. Lai, W.W. Zheng, H.W. Wang, W. Wang and M.W. Wang, *Energies,* 11(2018)2408.
3. H.B. Ren, Y.Z. Zhao, S.Z Chen and T.P. Wang, *Energy,* 166(2020)908.
4. J.Q. Zheng, Y.M. Xu, X. Gao, J.M. Zheng, H.Z. He and Z.G. Li, *Int. J. Electrochem. Sci.,*13(2018)11620.
5. D.J. Xuan, Z.F. Shi, J.Z. Chen, C.Y. Zhang and Y.X. Wang, *J. Clean. Prod.,* 252(2019)119787.

6. M.S.H. Lipu, M.A. Hannan, A. Hussain, M.M. Hoque, P.J. Ker, M.H.M. Saad and A. Ayo, *J. Clean. Prod.,* 205(2018)115.
7. E. Ferrero, S. Alessandrini and A. Balanzino, *Appl. Energ.,* 169(2016)450.
8. S.L. Wang, W. Tang, C. Fernandez, C.M. Yu, C.Y. Zou and X.Q. Zhang, *J. Clean. Prod.*, 210(2019)43.
9. J. Lv, S.L. Lin, W.J. Song, M.B. Chen, Z.P. Feng, Y.L. Li and Y.L. Ding, *Appl. Energ.*, 252(2019)113407.
10. K. Ramesh, C. Bharatiraja, S. Raghu, G. Vijayalakshmi and P.L. Sambanthan, *Int. J. Electron.,* 7(2016) 1261.
11. Y.X. Zhang, Z.J. Yang and C.X. Tian, *J. Mater. Chem. A*, 7 (2019)23628.
12. L.Z. Liu, S.L. Wang, F.L. Zhang, J.C. Pan and S.J. Pei, *Chinese Journal of Power Sources,* 42(2018) 25.
13. M. Song, Y. Hu, S.Y. Choe and T. R. Garrick, *J. Electrochem. Soc.,* 167(2020) 120503.
14. L.K.K. Maia, L. Drünert, F. Mantia and E. Zondervan, *J. Clean. Prod.,* 225(2019)928.
15. F.d. Zheng, Y.J. Xing, J.C. Jiang, B.X. Sun, J.H. Kim and M.Pecht, *Appl. Energ.,*183(2016)513.
16. Y.Tian, D.Li, J.D.Tian and B.Z.Xia, *Electrochimica Acta,* 225(2017)225.
17. Y.F. Ma, Y.X. Yang, L.W. Li, H.X. Liu and J. Shi, *Journal of Qingdao University(Engineering & Technology Edition),* 34(2019)58.
18. Environmental Idaho National Engineering and Laboratory, FreedomCAR Battery Test Manual For Power-Assist Hybrid Electric Vehicles, *Doe/Id-11069(2003) Draft*.
19. H.Q. Liu, Z.B. Wei, W.D. He and J.Y Zhao, *Energ.Convers.Manage.,* 150(2017)304.
20. A.S. Suleiman and D. Dennis, *J. Power Sources,* 130(2004)266.
21. X. Lei, X. Zhao, G.P. Wang and W.Y. Liu, *Energies,* 12(2019)3621.
22. Y.H. Hong, J.Q. Zheng, D.R. Deng, Q.H. Wu and W.F. Shen, *Int. J. Energy. Res.,*44(2020) 12112.
23. H.B. Luo, L.W. Deng, T.Y. Feng and C. Lv, *Energy Storage Science and Technology,* 6(2017)799